

# Quantum energy momentum tensor and equal time correlations in a Reissner-Nordström black hole

Roberto Balbinot\*

*Dipartimento di Fisica dell'Università di Bologna and INFN sezione di Bologna,  
Via Irnerio 46, 40126 Bologna, Italy*

Alessandro Fabbri<sup>†</sup>

*Departamento de Física Teórica and IFIC, Universidad de Valencia-CSIC,  
C. Dr. Moliner 50, 46100 Burjassot, Spain*



(Received 27 March 2023; accepted 24 July 2023; published 7 August 2023)

We consider a Reissner-Nordström black hole formed by the collapse of a charged null shell. The renormalized expectation values of the energy-momentum tensor operator for a massless scalar field propagating in the two-dimensional section of this spacetime are given. We then analyze the across-the-horizon correlations of the related energy density operator for free-falling observers to reveal the correlations between the Hawking particles and their interior partners.

DOI: [10.1103/PhysRevD.108.045004](https://doi.org/10.1103/PhysRevD.108.045004)

## I. INTRODUCTION

The existence of quantum correlations across the horizon in black holes (BHs) associated with Hawking radiation [1] has attracted increasing interest, especially in the community of analogue models [2]. As is well known, the Hawking effect consists in the conversion of quantum vacuum fluctuations in pairs of on-shell particles [3] (phonons in the case of acoustic black holes). A member of the pair (the Hawking particle) carries positive Killing energy and emerges outside the horizon and propagates to infinity, constituting the asymptotic thermal flux. The other member of the pair (the “partner”) has negative Killing energy and is created inside the horizon of the BH.

The correlations between the Hawking particle and its partner are a distinctive feature of the Hawking effect which should manifest itself in the appearance of a characteristic peak [4–6] in the equal-time correlation functions across the horizon; see Fig. 1. This peak has indeed been observed (see, for instance, Fig. 3(a) of Ref. [7]) in analogue BHs formed by a Bose-Einstein condensate (BEC) undergoing a transition from a subsonic flow to a supersonic one [7–9]. This remarkable fact represents up to today the best experimental evidence of the existence of Hawking radiation.

One should remark that the features of this correlation function highly depend on the fate of the partner and hence on the spacetime structure inside the horizon.

Note that in the acoustic BHs so far realized in the laboratory the supersonic region inside the horizon does not

end at a singularity, as in the gravitational case, but rather continues asymptotically towards a homogeneous configuration eventually reached by the partners. The presence of a central singularity, mimicked in the acoustic case by a sink absorbing both the condensate atoms and the phonons,<sup>1</sup> has a dramatic effect on the equal-time correlation functions: the peak does not appear (see Fig. 2). This is because the Hawking particles and their partners are created in a region of extension of the order of  $\frac{1}{\kappa}$ , where  $\kappa$  is the surface gravity of the BH, across the horizon, the so-called “quantum atmosphere” [10,11]. And when the Hawking particle emerges out of vacuum fluctuations from the quantum atmosphere, the corresponding partner has already been swallowed by the central singularity and no sign of correlations appears: they are lost in the singularity. To observe them, one has to consider correlations at unequal times in order to catch the partner before it disappears. These aspects have emerged in a recent study of the quantum correlations across the horizon in a Schwarzschild BH [6]. Given this strong dependence on the inner metric of the BH, here we extend the analysis to the case of a Reissner-Nordström (RN) BH whose internal structure, because of the presence of an inner horizon, is much more intriguing.

The plan of the paper is as follows. In Sec. II we present a simple model for the formation of a RN BH by the collapse of a null charged shell triggering the Hawking effect. In Sec. III, in preparation for the study of the quantum correlations across the horizon, we discuss the renormalized energy-momentum tensor associated with a massless

\*roberto.balbinot@unibo.it

†afabbri@ific.uv.es

<sup>1</sup>Experimental setups realizing these configurations are under construction. We thank I. Carusotto for this information.

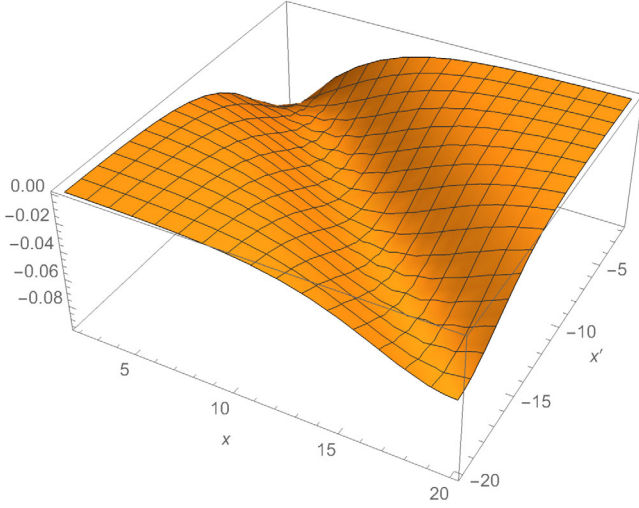


FIG. 1. Theoretically predicted equal-time density-density correlation function from the model in Refs. [5,6].  $x'$  is inside the horizon and  $x$  is outside. The peak is at  $x = -x'$ .

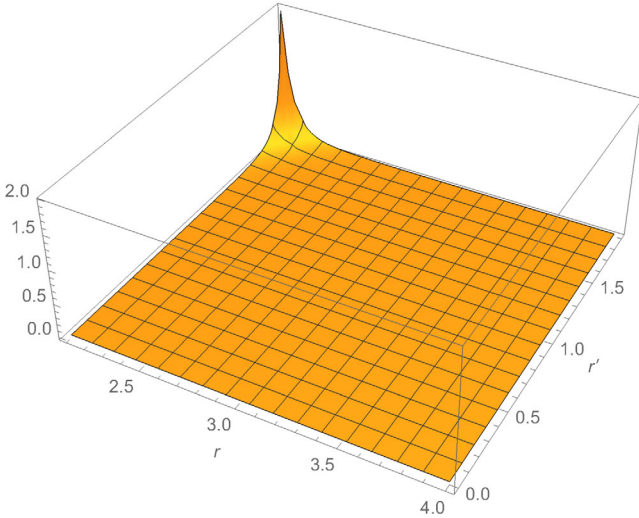


FIG. 2. Density-density correlation in the Schwarzschild black hole (see Ref. [6] for details), with  $r > 2m$  and  $r' < 2m$  ( $m = 1$ ).

scalar quantum field propagating in the two-dimensional section of the collapse spacetime of our model. We concentrate on the expectation value of the energy density operator as measured by a free-falling observer with particular attention to what happens close to the inner horizon. In Sec. IV we analyze the across-horizon correlation functions of the above energy density operator. Finally, Sec. V contains our conclusions.

## II. FORMING A REISSNER-NORDSTRÖM BH

It is well known that the formation of a BH triggers a vacuum instability leading to the emission of thermal radiation far away from the BH horizon. We use a simple

model for the formation of a RN BH, namely, the collapse of an ingoing charged null shell located at  $v = v_0$ , where  $v$  is an ingoing null coordinate.

The metric of the spacetime is of a Vaidya form,

$$ds^2 = -\left(1 - \frac{2m(r)}{r}\right)dv^2 + 2dvdr + r^2d\Omega^2, \quad (2.1)$$

where  $d\Omega^2 = d\theta^2 + \sin^2\theta d\varphi^2$  and  $m(r)$  is such that

$$m(r) = 0, \quad v < v_0, \quad (2.2)$$

$$m(r) = m - \frac{Q^2}{r}, \quad v > v_0. \quad (2.3)$$

For  $v < v_0$  the spacetime is Minkowski one and we can write the metric in a double null form,

$$ds^2 = -du_{\text{in}}dv + r^2(u_{\text{in}}, v)d\Omega^2, \quad (2.4)$$

where

$$r_{\text{in}} = \frac{v - u_{\text{in}}}{2} \quad (2.5)$$

and the double null coordinates are

$$u_{\text{in}} = t_{\text{in}} - r, \quad v = t_{\text{in}} + r. \quad (2.6)$$

In the future of the shell (i.e.,  $v > v_0$ ) the metric is the RN one which can also be given in a double null form,

$$ds^2 = -f(r)dudv + r^2d\Omega^2, \quad (2.7)$$

$$f(r) = 1 - \frac{2m}{r} + \frac{Q^2}{r^2}, \quad (2.8)$$

where

$$u = t - r^*, \quad v = t + r^*, \quad (2.9)$$

and  $r^*$  is the Regge-Wheeler tortoise coordinate

$$r^* = \int \frac{dr}{f} = r + \frac{1}{2\kappa_+} \ln |\kappa_-(r - r_+)| - \frac{1}{2\kappa_-} \ln |\kappa_-(r - r_-)|, \quad (2.10)$$

where

$$r_{\pm} = m \pm \sqrt{m^2 - Q^2} \quad (2.11)$$

are the two horizons and

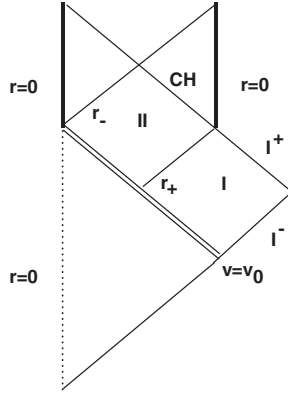


FIG. 3. Penrose diagram of the spacetime. The regions considered in this paper are the asymptotic one (I) and the one between the horizons (II).

$$\kappa_{\pm} = \frac{|f'(r)|_{r_{\pm}}}{2} = \frac{r_+ - r_-}{2r_{\pm}^2} = \frac{\sqrt{m^2 - Q^2}}{r_{\pm}^2} \quad (2.12)$$

are the corresponding surface gravities.

In order for Eq. (2.7) to describe a BH we require  $m^2 > Q^2$ . We refer to  $r_+$  (where  $u = +\infty$ ) simply as the event horizon of the BH, while we call the outgoing sheet of  $r_-$  (where  $u = -\infty$ ) the “inner horizon” and the ingoing one (where  $v = +\infty$ ) the “Cauchy horizon.” The relevant Penrose diagram is given in Fig. 3.

In regions I and II we introduce a time coordinate (Eddington-Finkelstein time) defined as

$$t_{\text{EF}} = v - r, \quad (2.13)$$

and

$$v = t_{\text{EF}} + r, \quad (2.14)$$

$$u = t_{\text{EF}} + r - 2r^* = t_{\text{EF}} - r - \frac{1}{\kappa_+} \ln |\kappa_+(r - r_+)| + \frac{1}{\kappa_-} \ln |\kappa_-(r - r_-)| \quad (2.15)$$

are RN null coordinates. Note that at the Cauchy horizon  $t_{\text{EF}}$  goes to  $+\infty$ . A spacetime diagram representing three characteristic curves  $u = cst$  in the RN portion of the spacetime is given in Fig. 4. The one denoted “Hawking particle” starts close outside the event horizon  $r_+$ , while the one denoted “partner” starts just inside  $r_+$ ; both are characterized by a large positive  $u$ . Another  $u = cst$  curve at intermediate  $u$  is also represented. Note the characteristic piling up of the  $u = cst$  trajectories along  $r_-$ . Finally, we also depict the trajectories of two free-falling observers crossing the event (and the inner) horizon at early time after the formation of the BH (observer A) and at late time (observer B).

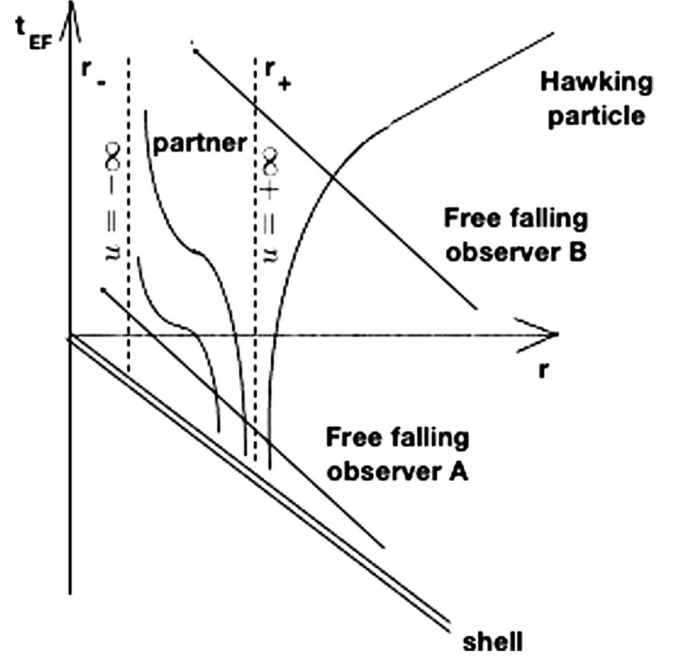


FIG. 4. Spacetime diagram in the RN portion of the spacetime representing three  $u = cst$  curves—one for the Hawking particle, one for the partner (both at large positive  $u$ ), and one for an intermediate value of  $u$ —and the trajectories of two free-falling observers crossing  $r_+$  and  $r_-$  at, respectively, early (observer A) and late time (observer B) after BH formation.

Matching the two line elements (2.4) and (2.7) along the shell  $v = v_0$ , we get [6]

$$u = u_{\text{in}} - \frac{1}{\kappa_+} \ln |\kappa_+(v_0 - u_{\text{in}} - 2r_+)| + \frac{1}{\kappa_-} \ln |\kappa_-(v_0 - u_{\text{in}} - 2r_-)|. \quad (2.16)$$

Using this, we can extend the  $u_{\text{in}}$  coordinate in the RN portion of the spacetime.

The event horizon ( $r = r_+$ ,  $u = +\infty$ ) corresponds to

$$u_{\text{in}}|_{\text{eh}} = v_0 - 2r_+ = 0. \quad (2.17)$$

To simplify the notation we set  $v_0 = 2r_+$  so that the event horizon ( $u = +\infty$ ) corresponds to  $u_{\text{in}} = 0$ . The inner horizon ( $u = -\infty$ ) corresponds to

$$u_{\text{in}}|_{\text{ih}} = 2(r_+ - r_-). \quad (2.18)$$

Equation (2.16) cannot be inverted analytically; however, we can get limiting behaviors near the event horizon (large positive  $u$ ),

$$u \simeq -\frac{1}{\kappa_+} \ln |-\kappa_+ u_{\text{in}}|, \quad (2.19)$$

and the inner horizon (large negative  $u$ ),

$$u \simeq \frac{1}{\kappa_-} \ln |\kappa_- (2(r_+ - r_-) - u_{\text{in}})|, \quad (2.20)$$

which will be useful in the rest of the paper. Note from these that  $u_{\text{in}}$  behaves in the limits considered as the Kruskal coordinate of the corresponding horizon.

### III. QUANTUM FIELD THEORY IN THE TWO-DIMENSIONAL RN SPACETIME

Now we consider a massless scalar quantum field  $\hat{\phi}$  propagating in the two-dimensional section ( $\theta = \varphi = cst$ ) of our collapse spacetime. Its equation of motion is

$$\hat{\square} \hat{\phi} = 0, \quad (3.1)$$

where  $\hat{\square} = \nabla_\mu \nabla^\mu$ . The field is supposed to be in a quantum state called  $|\text{in}\rangle$ , which corresponds to Minkowski vacuum on past null infinity (see Fig. 3), which is a Cauchy surface for our field equation.

Its energy-momentum tensor operator is

$$\hat{T}_{ab}(\hat{\phi}) = \partial_a \hat{\phi} \partial_b \hat{\phi} - \frac{g_{ab}}{2} \partial^c \hat{\phi} \partial_c \hat{\phi} \quad (3.2)$$

and the corresponding renormalized expectation values in the  $|\text{in}\rangle$  state are as follows (see Ref. [12] for details). For  $v < v_0$ ,

$$\langle \text{in} | \hat{T}_{ab} | \text{in} \rangle = 0. \quad (3.3)$$

For  $v > v_0$ ,

$$\begin{aligned} \langle \text{in} | \hat{T}_{vv} | \text{in} \rangle &= -\frac{1}{192\pi} (f'(r)^2 - 2f(r)f''(r)) \\ &= \frac{1}{24\pi} \left( -\frac{m}{r^3} + \frac{3(m^2 + Q^2)}{2r^4} - \frac{3mQ^2}{r^5} + \frac{Q^4}{r^6} \right) \\ &= \langle B | \hat{T}_{vv} | B \rangle, \end{aligned} \quad (3.4)$$

where a prime indicates a derivative with respect to  $r$ ,

$$\langle \text{in} | \hat{T}_{uu} | \text{in} \rangle = \langle B | \hat{T}_{uu} | B \rangle - \frac{1}{24\pi} \{u_{\text{in}}, u\}, \quad (3.5)$$

with  $\langle B | \hat{T}_{uu} | B \rangle = \langle B | \hat{T}_{vv} | B \rangle$  and  $\{, \}$  is the Schwarzian derivative calculated from Eq. (2.16). Explicitly,

$$\begin{aligned} \{u_{\text{in}}, u\} &= \frac{3}{2} \kappa_+^2 \frac{\left(1 - \frac{\kappa_+}{\kappa_-} \frac{u_{\text{in}}^2}{(u_{\text{in}} - 2(r_+ - r_-))^2}\right)^2}{\left(1 - \kappa_+ u_{\text{in}} - \frac{\kappa_+}{\kappa_-} \frac{u_{\text{in}}}{(u_{\text{in}} - 2(r_+ - r_-))}\right)^4} \\ &\quad - 2\kappa_+^2 \frac{\left(1 - \frac{\kappa_+}{\kappa_-} \frac{u_{\text{in}}^3}{(u_{\text{in}} - 2(r_+ - r_-))^3}\right)^2}{\left(1 - \kappa_+ u_{\text{in}} - \frac{\kappa_+}{\kappa_-} \frac{u_{\text{in}}}{(u_{\text{in}} - 2(r_+ - r_-))}\right)^3}. \end{aligned} \quad (3.6)$$

Finally,

$$\begin{aligned} \langle \text{in} | \hat{T}_{uv} | \text{in} \rangle &= \langle B | \hat{T}_{uv} | B \rangle \\ &= -\frac{1}{24\pi} \left(1 - \frac{2m}{r} + \frac{Q^2}{r^2}\right) \left(\frac{m}{r^3} - \frac{3Q^2}{2r^4}\right). \end{aligned} \quad (3.7)$$

Note that, because of conformal invariance,  $\hat{T}_{ab}$  is traceless, i.e.,  $\hat{T}_{uv} = 0$ . The nonvanishing result of Eq. (3.7) comes from the conformal anomaly, which in this case is simply proportional to the Ricci scalar. On the right-hand sides of Eqs. (3.4), (3.5), and (3.7) we have indicated the expectation values calculated in the Boulware vacuum  $|B\rangle$ , which describes the local vacuum polarization associated with the spacetime curvature. Note that at the horizons

$$\langle B | \hat{T}_{uu} | B \rangle|_{r_\pm} = \langle B | \hat{T}_{vv} | B \rangle|_{r_\pm} = -\frac{\kappa_\pm^2}{48\pi}. \quad (3.8)$$

The Schwarzian derivative in Eq. (3.5) is associated with the particle creation induced by the formation of the BH. These propagate along  $u = cst$  trajectories. Using the form of Eqs. (2.19) and (2.20), the following asymptotic behaviors of the Schwarzian derivative term can be found for  $u \rightarrow +\infty$  [ $u_{\text{in}} \rightarrow 0$  in Eq. (3.6)]:

$$-\frac{1}{24\pi} \{u_{\text{in}}, u\} = \frac{1}{48\pi} \kappa_+^2, \quad (3.9)$$

and

$$-\frac{1}{24\pi} \{u_{\text{in}}, u\} = \frac{1}{48\pi} \kappa_-^2 \quad (3.10)$$

for  $u \rightarrow -\infty$  [ $u_{\text{in}} \rightarrow 2(r_+ - r_-)$  in Eq. (3.6)]. A free-falling observer measures the following energy density associated with the field (see also Ref. [6]):

$$\rho = \langle \text{in} | \hat{\rho} | \text{in} \rangle = \langle \text{in} | \hat{T}_{ab} u^a u^b | \text{in} \rangle, \quad (3.11)$$

where  $u^a$  is the four-velocity vector of the observer's trajectory. One easily obtains

$$\begin{aligned} \hat{\rho} &= \frac{(E + \sqrt{E^2 - f})^2}{f^2} \langle \text{in} | \hat{T}_{uu} | \text{in} \rangle \\ &\quad + \frac{(E - \sqrt{E^2 - f})^2}{f^2} \langle \text{in} | \hat{T}_{vv} | \text{in} \rangle + \frac{2}{f} \langle \text{in} | \hat{T}_{uv} | \text{in} \rangle, \end{aligned} \quad (3.12)$$

where  $E$  is the conserved Killing energy of the observer. For the moment we set  $E = 1$ , which corresponds to a geodesic starting with zero velocity at infinity.

An exact analytical expression of  $\rho$  as a function of  $r$  and  $t_{\text{EF}}$  along the trajectory of the observer cannot be given since we are unable to invert Eq. (2.16) in order to express the Schwarzian derivative in terms of the above

coordinates. However, we can deduce some limiting behavior of  $\rho$ .

For an observer at infinity ( $r \rightarrow +\infty$ ) the vacuum polarization terms vanish, and if we consider the observer at late time ( $u \rightarrow +\infty$ ) we can use Eq. (3.9) and find

$$\rho = \frac{\kappa_+^2}{48\pi}, \quad (3.13)$$

which corresponds to a thermal flux of massless particles at the Hawking temperature,

$$T_H = \frac{\hbar\kappa_+}{2\pi}. \quad (3.14)$$

Now consider observers as they cross the event horizon  $r = r_+$ . First, let us rewrite Eq. (3.12) (for  $E = +1$ ) in the form

$$\rho = \frac{\left(1 + \sqrt{\frac{r_+ + r_-}{r} - \frac{r_+ r_-}{r^2}}\right)^2}{f^2} \langle \text{in} | \hat{T}_{uu} | \text{in} \rangle + \frac{\langle \text{in} | \hat{T}_{vv} | \text{in} \rangle}{\left(1 + \sqrt{\frac{r_+ + r_-}{r} - \frac{r_+ r_-}{r^2}}\right)^2} + \frac{2}{f} \langle \text{in} | \hat{T}_{uv} | \text{in} \rangle. \quad (3.15)$$

$$\rho = \frac{1}{48\pi} \left[ \frac{\left(1 + \sqrt{\frac{r_+ + r_-}{r} - \frac{r_+ r_-}{r^2}}\right)^2 r^2}{(r - r_-)^2} \left( \kappa_+^2 \left(1 + \frac{2r_+}{r} + \frac{3r_+^2}{r^2}\right) + \frac{\left(\frac{r_-^2}{r_+} - 3r_-\right)}{r^3} + \frac{2r_-^2}{r^4} \right) + \frac{-\frac{(r_+ + r_-)}{r^3} + \frac{3(r_+ + r_-)^2 + 3r_+ r_-}{r^4} - \frac{3r_+ r_- (r_+ + r_-)}{r^5} + \frac{2r_+^2 r_-^2}{r^6} - \frac{2(r_+ + r_-)}{r^3} + \frac{6r_+ r_-}{r^4}}{\left(1 + \sqrt{\frac{r_+ + r_-}{r} - \frac{r_+ r_-}{r^2}}\right)^2} \right], \quad (3.17)$$

giving the value

$$\rho|_{eh} = \frac{1}{48\pi} \left( \frac{6}{r_+^2} - \frac{6r_-}{\kappa_+ r_+^4} - \frac{\kappa_+^2}{4} - \frac{2(r_+ - 2r_-)}{r_+^3} \right) \quad (3.18)$$

on the event horizon.

The behavior of  $\rho$  as the observer approaches the inner horizon  $r_-$  is more delicate. If the observers cross the event horizon  $u = +\infty$  (and hence the inner horizon) at early time after the formation of the BH (see trajectory A in Fig. 4), they leave the large (positive)  $u$  region very rapidly and the measured energy density smoothly approaches the limiting value

$$\rho|_{ih} = \frac{1}{48\pi} \left( \frac{6}{r_-^2} - \frac{2}{\kappa_- r_+ r_-^2} - \frac{\kappa_-^2}{4} - \frac{2(r_- - 2r_+)}{r_-^3} \right). \quad (3.19)$$

Again, one sees the cancellation between the vacuum polarization (3.8) and (3.10).

To evaluate the Schwarzian derivative term entering  $\langle \text{in} | \hat{T}_{uu} | \text{in} \rangle$  one should note that the event horizon  $r_+$  corresponds to  $u = +\infty$  and in that limit, using again Eq. (3.9), we can write

$$\langle \text{in} | \hat{T}_{uu} | \text{in} \rangle = \langle B | \hat{T}_{uu} | B \rangle + \frac{\kappa_+^2}{48\pi} = \frac{1}{48\pi} \frac{(r - r_+)^2}{r^2} \left( \kappa_+^2 \left(1 + \frac{2r_+}{r} + \frac{3r_+^2}{r^2}\right) + \frac{\left(\frac{r_-^2}{r_+} - 3r_-\right)}{r^3} + \frac{2r_-^2}{r^4} \right), \quad (3.16)$$

which is exactly the value one would obtain in the Unruh vacuum associated with the event horizon. We see that it vanishes at  $r_+$ , making the first term in Eq. (3.15) finite as  $r \rightarrow r_+$ . The vacuum polarization piece [see Eq. (3.8)] is exactly canceled by the Schwarzian derivative one [see Eq. (3.9)]. The last term in Eq. (3.15) is also regular [see Eq. (3.7)], and putting everything together we can write

However, if the observer is approaching the inner horizon at very late time (trajectory B in Fig 4) things are strikingly different [13]. The outgoing null rays inside  $r_+$  peel away from the event horizon and asymptotically approach the inner horizon  $r_-$  (see Fig. 4) in a diverging  $t_{EF}$ . So, in the above limit the partners emitted just outside  $r_+$  with  $u \rightarrow +\infty$  get arbitrarily close to the inner horizon where  $f \ll 1$ . So at very late time our free-falling observers meet all of these partners in a region where  $f \ll 1$ , but  $u$  is still very large and positive. Using Eq. (3.9) for the Schwarzian derivative, we have that

$$\langle \text{in} | \hat{T}_{uu} | \text{in} \rangle = \langle B | \hat{T}_{uu} | B \rangle + \frac{\kappa_+^2}{48\pi}. \quad (3.20)$$

So the energy density they measure, in virtue of Eq. (3.8) evaluated at  $r_-$ , grows as  $\frac{\kappa_+^2 - \kappa_-^2}{f^2}$  coming from the first term in Eq. (3.15); the other two are bounded. Since  $\kappa_- > \kappa_+$ , this ever-increasing density is negative.

Finally, we can consider the case of an observer approaching the Cauchy horizon starting from inside the event horizon. For this observer  $E$  is negative, say,  $E = -1$ , and Eq. (3.15) is replaced by

$$\rho = \frac{\langle \text{in} | \hat{T}_{uu} | \text{in} \rangle}{\left(1 + \sqrt{\frac{r_+ + r_-}{r} - \frac{r_+ r_-}{r^2}}\right)^2} + \frac{\left(1 + \sqrt{\frac{r_+ + r_-}{r} - \frac{r_+ r_-}{r^2}}\right)^2}{f^2} \times \langle \text{in} | \hat{T}_{vv} | \text{in} \rangle + \frac{2}{f} \langle \text{in} | \hat{T}_{uv} | \text{in} \rangle, \quad (3.21)$$

showing that  $\rho$  diverges as  $-\frac{\kappa_-^2}{f^2}$  due to vacuum polarization.

#### IV. PARTICLE-PARTNER CORRELATIONS

The analysis of the expectation values of the energy-momentum tensor operator in the last section has shown how vacuum polarization effects and particle creation mix and, beside kinematical effects associated with the world line of the observer, both contribute to the measured energy density. The energy-momentum tensor only asymptotically describes an outgoing flux of particles at the Hawking temperature. On the other hand, inside the horizon, because of the nonvanishing vacuum polarization, the tensor does not simply describe an ingoing flux of partners. To reveal the genuine pair-creation process, which is the basis of the Hawking effect, one should try to highlight the existing quantum correlations between the Hawking particles and their associated partners. To this end, in this section we discuss the correlation functions  $G(x, x')$  of the energy density operator

$$G(x, x') \equiv \langle \text{in} | \hat{\rho}(x) \hat{\rho}(x') | \text{in} \rangle, \quad (4.1)$$

where

$$\hat{\rho} = \frac{(E + \sqrt{E^2 - f})^2}{f^2} \hat{T}_{uu} + \frac{(E - \sqrt{E^2 - f})^2}{f^2} \hat{T}_{vv} \quad (4.2)$$

and  $\hat{T}_{ab}$  is the energy-momentum tensor operator defined in Eq. (3.2).  $E$  is the conserved Killing energy of the observer. The starting point is the two-point function for the  $|\text{in}\rangle$  vacuum,

$$\langle \text{in} | \hat{\phi}(x) \hat{\phi}(x') | \text{in} \rangle = -\frac{\hbar}{4\pi} \ln(u_{\text{in}} - u'_{\text{in}})(v - v'). \quad (4.3)$$

From this, one can build the fundamental object of our calculation,

$$\partial_u \partial_{u'} \langle \text{in} | \hat{\phi}(x) \hat{\phi}(x') | \text{in} \rangle = -\frac{\hbar}{4\pi} \frac{du_{\text{in}}}{du} \frac{du'_{\text{in}}}{du'} \frac{1}{(u_{\text{in}} - u'_{\text{in}})^2}. \quad (4.4)$$

The  $\hat{T}_{uu}$  correlator is then (see Ref. [6] for details)

$$\langle \text{in} | \hat{T}_{uu}(x) \hat{T}_{uu}(x') | \text{in} \rangle = [\partial_u \partial_{u'} \langle \text{in} | \hat{\phi}(x) \hat{\phi}(x') | \text{in} \rangle]^2. \quad (4.5)$$

This is the relevant one to discuss the Hawking-partner correlations.

We can write the density correlator as follows (both observers have  $E = +1$ ):

$$G(x, x') = \frac{\langle \text{in} | \hat{T}_{uu}(x) \hat{T}_{u'u'}(x') | \text{in} \rangle}{\left(1 - \sqrt{\frac{2m(r)}{r}}\right)^2 \left(1 - \sqrt{\frac{2m(r')}{r}}\right)^2} + \frac{\langle \text{in} | \hat{T}_{vv}(x) \hat{T}_{v'v'}(x') | \text{in} \rangle}{\left(1 + \sqrt{\frac{2m(r)}{r}}\right)^2 \left(1 + \sqrt{\frac{2m(r')}{r}}\right)^2}. \quad (4.6)$$

As said before, for our purposes we focus on the first term in Eq. (4.6), taking the point  $x$  outside the event horizon  $r_+$  and  $x'$  in between the inner horizon and the event horizon.

Consider first a trajectory of our inner observer like the one labeled  $A$  in Fig. 2 and take  $x'$  inside and close to  $r_+$ . We can then use Eq. (2.19), namely,

$$u' \sim -\frac{1}{\kappa_+} \ln | -\kappa_+ u'_{\text{in}} |. \quad (4.7)$$

Similarly, taking  $x$  close outside  $r_+$ , and again using Eq. (2.19),

$$u \sim -\frac{1}{\kappa_+} \ln | -\kappa_+ u_{\text{in}} |. \quad (4.8)$$

Inserting these into Eq. (4.4), we have

$$\frac{\langle \text{in} | \hat{T}_{uu}(x) \hat{T}_{u'u'}(x') | \text{in} \rangle}{\left(1 - \sqrt{\frac{2m(r)}{r}}\right)^2 \left(1 - \sqrt{\frac{2m(r')}{r}}\right)^2} \sim \frac{1}{\left(1 - \sqrt{\frac{2m(r)}{r}}\right)^2 \left(1 - \sqrt{\frac{2m(r')}{r}}\right)^2} \left( \frac{\hbar \kappa_+^2}{16\pi \cosh^2\left(\frac{\kappa_+}{2}(u - u')\right)} \right)^2. \quad (4.9)$$

One sees the appearance of the well-known  $\cosh^2$  term modulated by the geometrical prefactors containing  $\sqrt{\frac{2m(r)}{r}}$ . For an acoustic BH in a BEC the density-density correlator has a similar structure to Eq. (4.9) (more precisely, the

square of it). In that case, the points  $x$  and  $x'$  are typically taken far away on both sides of the acoustic (single) horizon where the medium is homogeneous and the geometric prefactors are just harmless constants, and the peak of the correlator corresponds to the maximum of the  $\cosh^{-2}$  term,

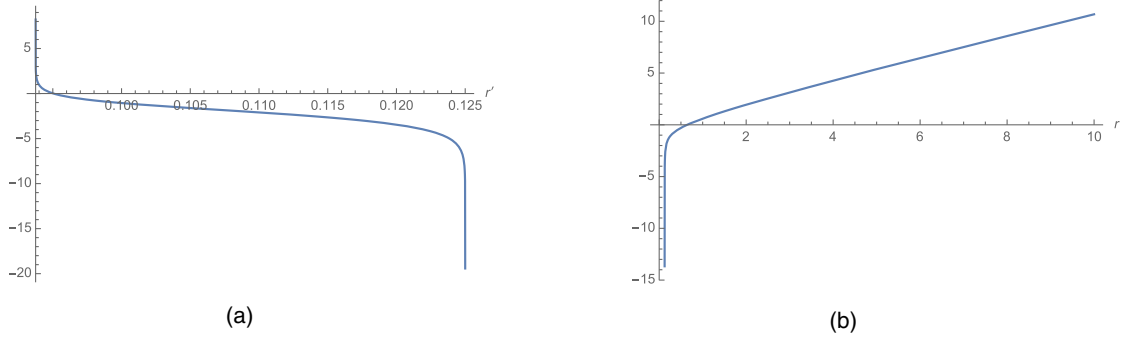


FIG. 5. Plot of the left-hand side (a) and right-hand side (b) of Eq. (4.10). In this figure and those that follow, we consider  $r_+ = \frac{1}{8} = 0.125$ ,  $r_- = \frac{3}{32} = 0.09375$ ,  $\kappa_+ = 1$ , and  $\kappa_- = \frac{16}{9}$ .

namely,  $u = u'$ , i.e., along the trajectories of the Hawking particle and its corresponding partner. This condition at equal time in our case would be

$$\begin{aligned} r' + \frac{1}{\kappa_+} \ln |\kappa_+(r' - r_+)| - \frac{1}{\kappa_-} \ln |\kappa_-(r' - r_+)| \\ = r + \frac{1}{\kappa_+} \ln |\kappa_+(r - r_+)| - \frac{1}{\kappa_-} \ln |\kappa_-(r - r_+)|, \end{aligned} \quad (4.10)$$

where remember that  $r_- < r' < r_+$  and  $r > r_+$ . The plot of Eq. (4.10) is given in Fig. 5: they both go to  $+\infty$  for both  $r \rightarrow r_-$  and  $r \rightarrow +\infty$  and to  $-\infty$  for  $r \rightarrow r_+$ .

From these, one sees that the condition (4.10) can always be satisfied, i.e., for every  $r > r_+$  a value of  $r'$  exists such that  $r_- < r' < r_+$  and Eq. (4.10) is satisfied. However, if we plot the correlator (4.9) for both points close to  $r_+$ , no sign of the particle-partner correlation appears. In Fig. 6 the correlator (4.9) is represented graphically at values of  $r'$

fixed as a function of  $r$ , while in Fig. 7 the three-dimensional plot is shown. The reason for this behavior is that correlations only appear when the particles and the partners emerge out of the quantum atmosphere.<sup>2</sup>

Looking at Fig. 5, one sees that all points with  $r - r_+ \geq \frac{1}{\kappa_+}$  are correlated with corresponding partners located very close to  $r_-$ , so let us consider the inner point  $r'$  in this region. We have to distinguish two regimes. If the inner observer approaches the inner horizon  $r_-$  at early time with respect to the formation of the BH (trajectory A in Fig. 4), we have that the corresponding  $u'$  approaches  $-\infty$  as

$$u' \sim \frac{1}{\kappa_-} \ln |\kappa_-(2(r_+ - r_-) - u'_{\text{in}})|. \quad (4.11)$$

If we take the other observer in the region  $u \rightarrow +\infty$ , using Eqs. (4.11) and (4.8) the correlator is given by

$$\begin{aligned} \frac{\langle \text{in} | \hat{T}_{uu}(x) \hat{T}_{u'u'}(x') | \text{in} \rangle}{\left(1 - \sqrt{\frac{2m(r)}{r}}\right)^2 \left(1 - \sqrt{\frac{2m(r')}{r'}}\right)^2} \sim \frac{1}{\left(1 - \sqrt{\frac{2m(r)}{r}}\right)^2 \left(1 - \sqrt{\frac{2m(r')}{r'}}\right)^2} \\ \times \frac{(\hbar \kappa_+^2 \kappa_-^2)^2}{\left(4\pi \left(2\kappa_+ \kappa_- (r_+ - r_-) e^{\frac{\kappa_+ u - \kappa_- u'}{2}} - \kappa_+ e^{\frac{\kappa_+ u + \kappa_- u'}{2}} + \kappa_- e^{-\frac{\kappa_+ u + \kappa_- u'}{2}}\right)^2\right)^2}, \end{aligned} \quad (4.12)$$

which has a more complicated structure than the one in Eq. (4.9). Note that, using Eq. (2.15), the correlator (4.12), unlike Eq. (4.9), is time dependent. We graphically represent this correlator fixing the inner point very close to  $r_-$  in Fig. 8, and the three-dimensional plot is shown in Fig. 9. Again, no sign of the correlations appears. The reason for this is clear from Fig. 4.

The partners of the Hawking particles pile up at  $r_-$  and only at late time are they intercepted by our inner observer close to  $r_-$  (see trajectory B in Fig. 4). So in order to reveal the correlation we have to consider the limit in which  $u'$  is given by Eq. (4.7) and  $r'$  is close to  $r_-$ . The correlator is

given by Eq. (4.9) with  $r' \rightarrow r_-$  and the corresponding plots are shown in Figs. 10 and 11. We see clearly the appearance of the foreseen peak. The corresponding  $r$  is not exactly the one given by Eq. (4.10) because of the nontrivial role played by the geometric prefactor containing  $\sqrt{\frac{2m(r)}{r}}$ .

The situation in which the inner observer approaches the Cauchy horizon is completely different. In that case, since

<sup>2</sup>Close to the horizon, the correlator is dominated by the light-cone singularity (coincidence limit in the case of equal time).

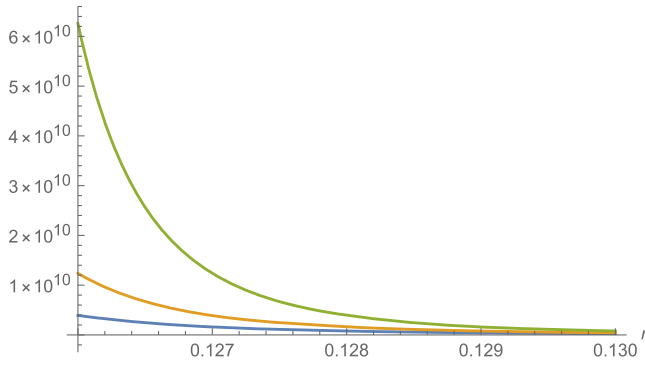


FIG. 6. Plot of the correlator (4.9), up to the factor  $(\frac{\hbar}{4\pi})^2$ , as a function of  $r$  for fixed values of  $r' = 0.122$  (blue),  $0.123$  (orange), and  $0.124$  (green).

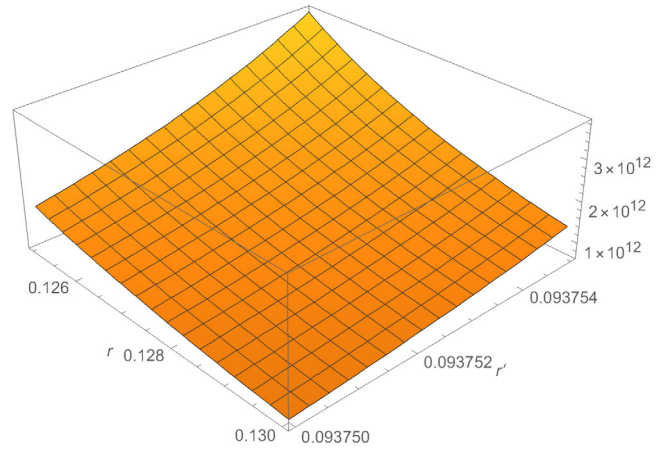


FIG. 9. Three-dimensional plot of the correlator (4.12), up to the factor  $(\frac{\hbar}{4\pi})^2$ , for  $t_{\text{EF}} = 1$ ,  $0.09375 < r' < 0.093755$  and  $0.125 < r < 0.130$ .

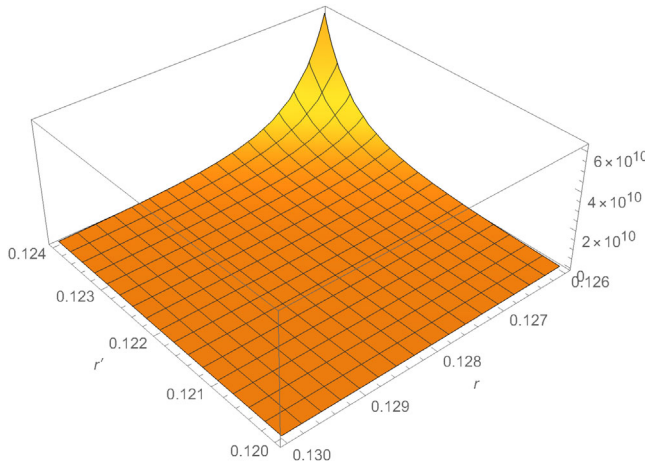


FIG. 7. Three-dimensional plot of the correlator (4.9), up to the factor  $(\frac{\hbar}{4\pi})^2$ , for  $0.120 < r' < 0.124$  and  $0.126 < r < 0.130$ .

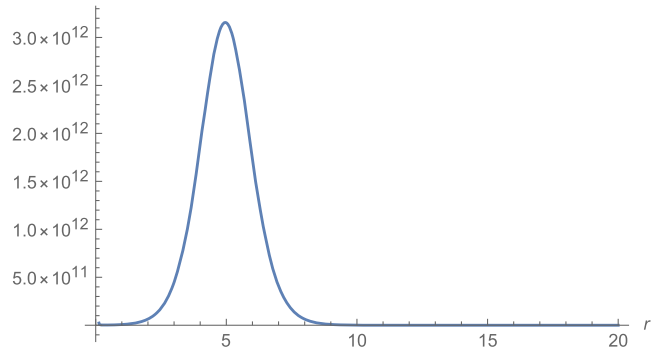


FIG. 10. Plot of the correlator (4.9), up to the factor  $(\frac{\hbar}{4\pi})^2$ , with the inner point fixed at  $r' = 0.0937501$  and as a function of  $r$ ,  $0.125 < r < 20$ .

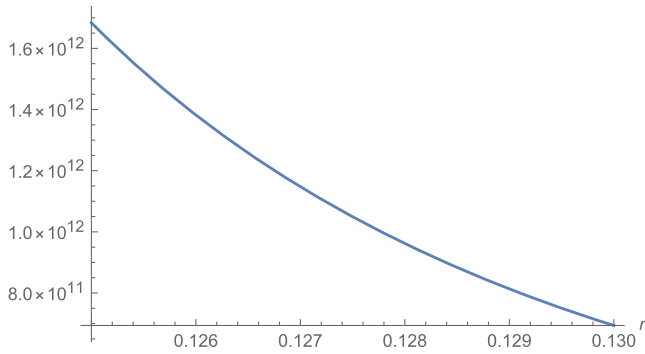


FIG. 8. Plot of the correlator (4.12), up to the factor  $(\frac{\hbar}{4\pi})^2$ , for  $t_{\text{EF}} = 1$ , with the inner point fixed at  $r' = 0.0937501$  and as a function of  $r$ ,  $0.125 < r < 0.130$ .

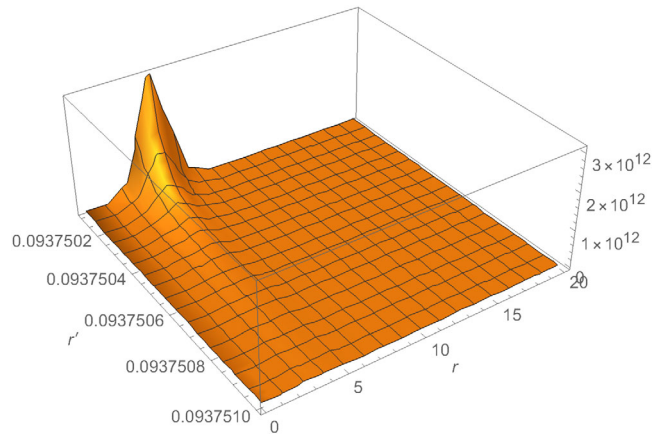


FIG. 11. Three-dimensional plot of the correlator (4.9), up to the factor  $(\frac{\hbar}{4\pi})^2$ , for  $0.0937501 < r' < 0.093751$  and  $0.125 < r < 20$ .



this observer has  $E = -1$  [see Eq. (4.2)] the  $G(x, x')$  correlator becomes

$$G(x, x') = \frac{\langle \text{in} | \hat{T}_{uu}(x) \hat{T}_{u'u'}(x') | \text{in} \rangle}{\left(1 - \sqrt{\frac{2m(r)}{r}}\right)^2 \left(1 + \sqrt{\frac{2m(r')}{r'}}\right)^2} + \frac{\langle \text{in} | \hat{T}_{vv}(x) \hat{T}_{v'v'}(x') | \text{in} \rangle}{\left(1 + \sqrt{\frac{2m(r)}{r}}\right)^2 \left(1 - \sqrt{\frac{2m(r')}{r'}}\right)^2}, \quad (4.13)$$

and the dominant, now diverging contribution comes from the last term, namely, the  $\hat{T}_{vv}$  correlator,

$$\frac{\langle \text{in} | \hat{T}_{vv}(x) \hat{T}_{v'v'}(x') | \text{in} \rangle}{\left(1 + \sqrt{\frac{2m(r)}{r}}\right)^2 \left(1 - \sqrt{\frac{2m(r')}{r'}}\right)^2} \sim \frac{1}{\left(1 + \sqrt{\frac{2m(r)}{r}}\right)^2 \left(1 - \sqrt{\frac{2m(r')}{r'}}\right)^2} \left(\frac{\hbar}{4\pi(v - v')}\right)^2, \quad (4.14)$$

showing explicitly the divergence as  $r' \rightarrow r_-$  due to the vacuum polarization.

## V. CONCLUSIONS

In this paper, within the framework of quantum field theory in curved spacetime, we studied, in a two-dimensional section of the RN BH spacetime formed by the collapse of a null shell, the expectation values of the energy-momentum tensor operator for a massless scalar field, showing how vacuum polarization and particle creation mix and one cannot disentangle the two; both contribute to the measured energy density. Only sufficiently far away from the horizon, the tensor describes an outgoing flux of particles at the Hawking temperature. To reveal the existing correlations between Hawking particles and their partners, one has to look at correlation functions.

By studying equal-time correlators in a Schwarzschild BH, we found [6] that the above correlations do not show up because the partner is swallowed by the central singularity before the correlated Hawking particle emerges from the quantum atmosphere. To reveal the correlations, one has to consider unequal-time correlators in order to catch the partner before it disappears into the singularity.

In a RN BH the picture changes significantly. The spacetime structure inside the event horizon is characterized by the presence of an inner horizon before reaching the singularity. At this horizon, all of the partners pile up asymptotically, never reaching the singularity. So, at late time, equal-time correlators across the horizon provide a significant enhancement when the inner point is taken close to the inner horizon, singling out the quantum entanglement of the Hawking particles and the partners. On the ingoing part of the inner horizon (the Cauchy horizon), on the other hand, we found that the correlators diverge like the energy-momentum tensor, with the divergence being caused by infinite vacuum polarization there.

We should stress that our analysis is restricted to the gravitational case discussed within the framework of Einstein's general relativity. In acoustic BHs realized with BECs, because of the modified dispersion relation that allows for "superluminally" propagating modes, the partners do not pile up at the inner horizon, but rather bounce back and forth between the inner and event horizons, producing the so-called laser effect [14] which, in turn, causes the rise of a dynamical instability [15].

## ACKNOWLEDGMENTS

A.F. acknowledges partial financial support by the Spanish Ministerio de Ciencia e Innovación Grant No. PID2020-116567GB-C21 funded by Grant No. MCIN/AEI/10.13039/501100011033, and the Project No. PROMETEO/2020/079 (Generalitat Valenciana).

- 
- [1] S. W. Hawking, *Nature (London)* **248**, 30 (1974); *Commun. Math. Phys.* **43**, 199 (1975).
  - [2] C. Barcelo, S. Liberati, and M. Visser, *Living Rev. Relativity* **8**, 12 (2005).
  - [3] R. Brout, S. Massar, R. Parentani, and P. Spindel, *Phys. Rep.* **260**, 329 (1995).
  - [4] R. Balbinot, A. Fabbri, S. Fagnocchi, A. Recati, and I. Carusotto, *Phys. Rev. A* **78**, 021603 (2008).
  - [5] A. Fabbri and R. Balbinot, *Phys. Rev. Lett.* **126**, 111301 (2021).
  - [6] R. Balbinot and A. Fabbri, *Phys. Rev. D* **105**, 045010 (2022).
  - [7] J.R.M. de Nova, K. Golubkov, V.I. Kolobov, and J. Steinhauer, *Nature (London)* **569**, 688 (2019).
  - [8] J. Steinhauer, *Nat. Phys.* **12**, 959 (2016).
  - [9] V.I. Kolobov, K. Golubkov, J.R.M. de Nova, and J. Steinhauer, *Nat. Phys.* **17**, 362 (2021).
  - [10] S.B. Giddings, *Phys. Lett. B* **754**, 39 (2016).
  - [11] R. Dey, S. Liberati, Z. Mirzaiyan, and D. Pranzetti, *Phys. Lett. B* **797**, 134828 (2019).
  - [12] R. Balbinot, A. Fabbri, S. Farese, and R. Parentani, *Phys. Rev. D* **76**, 124010 (2007).
  - [13] T. Jacobson, *Phys. Rev. D* **57**, 4890 (1998).
  - [14] S. Corley and T. Jacobson, *Phys. Rev. D* **59**, 124011 (1999).
  - [15] A. Coutant and R. Parentani, *Phys. Rev. D* **81**, 084042 (2010).